

# The European Muon Collaboration effect in Light-Front Hamiltonian Dynamics

Emanuele Pace,<sup>1</sup> Matteo Rinaldi,<sup>2</sup> Giovanni Salmè,<sup>3</sup> and Sergio Scopetta<sup>2</sup>

<sup>1</sup>*Università di Roma “Tor Vergata”, Via della Ricerca Scientifica 1, 00133 Rome, Italy*

<sup>2</sup>*Dipartimento di Fisica e Geologia, Università degli Studi di Perugia and Istituto Nazionale di Fisica Nucleare, Sezione di Perugia, via A. Pascoli, I - 06123 Perugia, Italy*

<sup>3</sup>*Istituto Nazionale di Fisica Nucleare, Sezione di Roma, Piazzale A. Moro 2, 00185 Rome, Italy*

A rigorous light-front formalism for electron deep inelastic scattering on unpolarized nuclei, in Bjorken limit, is reported. It preserves Poincaré covariance, macroscopic locality, both number of particles and momentum sum rules. The scheme is applied to the  $A=3$  iso-doublet, very relevant in view of the planned operation with unpolarized and polarized beams at the Electron-Ion Collider. At variance with previous light-front estimates, our procedure, including a realistic nuclear description and free-nucleon structure functions, predicts a sizeable European Muon Collaboration effect for  ${}^3\text{He}$ . This will allow to analyze deviations from the proposed baseline in terms of genuine QCD effects. The extension to heavier nuclei is straightforward, although numerically challenging.

After almost forty years of studies, the European Muon Collaboration (EMC) effect [1], with the characteristic depletion of the ratio  $R_{EMC}^A(x)$  between electron-nucleus and electron-deuterium deep inelastic scattering (DIS) cross sections (normalized to the relative number of nucleons) in the intermediate region of the Bjorken variable  $x$ , has not yet been fully understood. Any attempt to explain the electromagnetic (em) response of the nucleus in the DIS kinematic region simply as the incoherent response of the *constituent* nucleons, assumed to be the only degrees of freedom (dof) acting in the nucleus, failed to succeed. This finding raised the question about how and to what extent the nucleus can be considered as a QCD laboratory, where quark and gluon dof's play a significant role. Unfortunately, a quantitative answer is still lacking, although important progresses have been made, e.g. by determining the role of the short-range correlations between the nucleons once the nucleus is probed by high-virtuality photons [2–4], and also by addressing the medium modification of the nucleons, given the large overlap between them (see, e.g. Ref. [5]). Perhaps, the answer could be found in the study of complementary semi-inclusive and exclusive processes [6], planned for light nuclei at existing [7] and future [8] high-energy facilities, like the Electron-Ion Collider (EIC), where a relevant program of measurements with (polarized)  ${}^3\text{He}$  beams is under development. For now, new  ${}^3\text{He}$  and  ${}^3\text{H}$  DIS data have been taken at JLab by the MARATHON Collaboration [9] allowing a fresh extraction of the ratio of the neutron to proton structure functions (SFs)  $r(x) = F_2^n(x)/F_2^p(x)$ , needed for the flavor decomposition (see also Ref. [10]). This experimental scenario has motivated our efforts to improve the quantitative analysis of the EMC effect for the bound three-nucleon systems.

In order to make highly reliable search and discovery of effects that can explain the EMC results, one should first establish a sound baseline, which means i) embedding general principles to the greatest extent and ii) including the very successful description of nuclei, elaborated by phenomenologists over decades. In view of this, we

propose a Poincaré-covariant formalism for nuclear DIS without medium deformations of the bound nucleons, but fully able to exploit the sophisticated description of nuclei, as achieved nowadays. The approach, to be applied to the nuclear SFs, has been carefully developed for  ${}^3\text{He}$  in Ref. [11] within the light-front Hamiltonian dynamics (LFHD) [12, 13] (the most suitable when an em probe is used), and it is valid for any nucleus. A Poincaré-covariant description of nuclei and in particular of  ${}^3\text{He}$  will have a remarkable impact on the interpretation of the experimental results at the EIC, where a crucial part of the program will involve light-ion beams (see, e.g., sections 2.6, 2.7, 7.2, 7.3 of Ref. [8]).

The main ingredient is the light-front (LF) spectral function [14],  $\mathcal{P}^N(\vec{\kappa}, \epsilon)$ , the probability distribution of finding a nucleon with LF momentum  $\vec{\kappa}$ <sup>1</sup> in the intrinsic reference frame of the cluster  $[1, (A-1)]$  and the fully interacting  $(A-1)$ -nucleon system with intrinsic energy  $\epsilon$ . In particular, notice that we use nonsymmetric intrinsic variables, which disentangle the internal motion of the interacting  $(A-1)$ -nucleon system from that of the struck nucleon and hence are able to implement the macroscopic locality [13]. Recently, in this framework, the six  ${}^3\text{He}$  leading-twist transverse-momentum distributions have been evaluated in valence approximation [15].

In what follows, adopting the Bjorken limit, we first introduce the unpolarized nuclear SF,  $F_2^A(x)$ , (see also Ref. [11]), and show novel spin-independent and spin-dependent light-cone momentum distributions. To evaluate the nuclear SF, according to our final goal, we have to adopt the free-nucleon SFs, for which many parametrizations exist. To minimize the dependence upon the chosen nucleon SFs and test the self-consistency of our approach, we extract  $r(x)$  from the experimental DIS cross-sections off  ${}^3\text{He}$  and  ${}^3\text{H}$  nuclei [9], by applying the itera-

<sup>1</sup> The light-front components of a four vector  $v$  are  $(v^-, \vec{v})$ , where  $\vec{v} = (v^+, \mathbf{v}_\perp)$  with  $v^\pm = v^0 \pm \hat{\mathbf{n}} \cdot \mathbf{v}$  and  $\mathbf{v}_\perp = \mathbf{v} - \hat{\mathbf{n}}(\hat{\mathbf{n}} \cdot \mathbf{v})$ . The vector  $\hat{\mathbf{n}}$  is a generic unit vector. In this paper we choose  $\hat{\mathbf{n}} \equiv \hat{z}$ .

tive method of Refs. [16, 17] and our Poincaré-covariant expression of the SF  $F_2^{A=3}$ . Finally from  $r(x)$  and the proton SF  $F_2^p(x)$  of Ref. [18] the EMC ratio,  $R_{EMC}^{A=3}(x)$ , is evaluated and compared with existing experimental data.

It is very important to notice that previous calculations elaborated within the LF dynamics did not predict any EMC effect, i.e. it was obtained  $R_{EMC}^A(x) \geq 1$ , as discussed, e.g., in Refs. [19, 20]. More precisely, it is generally thought that the EMC effect cannot be explained by unmodified nucleons only (see, e.g., Refs. [2, 3], for the in-medium modifications). However, notice that in Refs. [19, 20] a nuclear mean field is used, so that the nuclear correlations are not properly treated. In addition, in Refs. [21, 22] LF calculations with symmetric intrinsic variables were performed and covariance was only assured for kinematical Lorentz transformations. Therefore, accurate studies of the EMC effect within a Poincaré-covariant framework, enriched by a sound dynamical content, are mandatory. For the latter purpose, in this work the three-body wave functions (wfs) [23, 24], obtained from the NN charge-dependent Av18 potential [25] (including the Coulomb interaction) plus the NNN Urbana IX force [26], are used.

*Formalism.* We adopt the reference frame where the nucleus three-momentum is  $\mathbf{P}_A = 0$  and the four-momentum transfer has components:  $q \equiv \{q_0, q_z = -|\mathbf{q}|, \mathbf{0}_\perp\}$ . Moreover, we assume the impulse approximation (IA), that is suitable for describing a high-virtuality photon that impinges on a nucleon inside the nucleus, leaving unaffected the fully interacting spectator system. In Ref. [27] it was shown that the IA satisfies the covariance with respect to Poincaré transformations plus time reversal and parity, if applied in the Breit frame with the momentum transfer  $\mathbf{q}_\perp = 0$  and in any frame reachable through a LF boost parallel to the  $z$  axis. In IA, one obtains the following general expression of the nuclear SF (see Ref. [11])

$$F_2^A(x) = \sum_N \int d\epsilon \int \frac{d\mathbf{k}_\perp}{(2\pi)^3} \int_{\xi_{min}^B}^1 d\xi \frac{\mathcal{P}^N(\tilde{\mathbf{k}}, \epsilon) E_S}{2 \kappa^+ (1 - \xi)} F_2^N(z), \quad (1)$$

where i)  $\tilde{\mathbf{k}} \equiv \{\kappa^+, \mathbf{k}_\perp\}$ , with  $\kappa^+ = \xi \mathcal{M}_0(1, A - 1)$  and  $\mathcal{M}_0(1, A - 1)$  the free mass of the cluster  $[1, (A - 1)]$ ; ii)  $E_S = \sqrt{M_S^2 + |\mathbf{k}_\perp|^2 + |\boldsymbol{\kappa}_z|^2}$  is the total energy of the  $(A - 1)$ -nucleon spectator system (see Eq. (46) in Ref. [14] for the expression of  $\kappa_z$ ), with  $M_S = (A - 1)m + \epsilon$  the mass of the interacting  $(A - 1)$ -nucleon system,  $\epsilon$  its intrinsic energy and  $m$  the nucleon mass; iii)  $z = Q^2/(2p \cdot q)$  with  $p$  the off-shell nucleon four-momentum.

In the Bjorken limit, one can readily exchange the integrations on  $\epsilon$  and  $\mathbf{k}_\perp$  and the integration on  $\xi$ , since both  $z = \xi_{min}^B/\xi$  and  $\xi_{min}^B = x m/M_A$  do not depend on  $\epsilon$  and  $\mathbf{k}_\perp$ . Then the nuclear SF becomes

$$F_2^A(x) = \sum_N \int_{\xi_{min}^B}^1 d\xi F_2^N(z) f_1^N(\xi), \quad (2)$$

where  $f_1^N(\xi)$  is the unpolarized light-cone momentum distribution given by

$$f_1^N(\xi) = \int d\mathbf{k}_\perp n^N(\xi, \mathbf{k}_\perp), \quad (3)$$

with  $n^N(\xi, \mathbf{k}_\perp)$  the LF spin-independent nucleon momentum distribution (see Refs. [14, 15]), viz.

$$n^N(\xi, \mathbf{k}_\perp) = \int d\epsilon \frac{\mathcal{P}^N(\tilde{\mathbf{k}}, \epsilon)}{(2\pi)^3 2 \kappa^+} \frac{E_S}{(1 - \xi)}. \quad (4)$$

This quantity is the trace of the momentum-distribution  $2 \times 2$  matrix,  $\mathcal{N}_{\mathcal{M}}^N(\xi, \mathbf{k}_\perp, \mathbf{S})$  [15], with  $\mathbf{S}$  the polarization of the nucleus and  $\mathcal{M}$  the component of the total angular momentum  $\mathcal{J}$  along  $\mathbf{S}$  (in general  $\mathbf{S} \neq \hat{z}$ ). The trace is obviously independent of  $\mathbf{S}$  and  $\mathcal{M}$ . It is worth noticing that, in our Poincaré-covariant framework, the momentum distribution fulfills both normalization (i.e. the baryon number sum rule) and momentum sum rule [14, 15]. Finally, in the Bjorken limit, the evaluation of the nuclear SF is simplified, since  $n^N(\xi, \mathbf{k}_\perp)$  can be obtained more directly from the nucleus wf in momentum space [15], rather than through the cumbersome LF spectral-function. Hence, once the ground-state of a nucleus is calculated with a realistic interaction, the corresponding nuclear structure function can be affordably evaluated in the Bjorken limit, through Eqs. (2) and (3). Differently, for describing the nuclear DIS in IA, one needs the knowledge of the LF spectral function  $\mathcal{P}^N(\tilde{\mathbf{k}}, \epsilon)$  [11].

For  $A = 3$ , Eq. (4), in terms of the wf in momentum space,  $\mathcal{G}_{L\rho X}^{j_{23}l_{23}s_{23}}(k_{23}, k)$ , reads [15]

$$n^N(\xi, \mathbf{k}_\perp) = \sum_{T_{23}, \tau_{23}} \langle T_{23} \tau_{23} | \frac{1}{2} \tau | \frac{1}{2} T_z \rangle^2 \int_0^\infty dk_{23} k_{23}^2 \times \frac{E_{23} E(\mathbf{k})}{4\pi (1 - \xi) k^+} \sum_{j_{23}, l_{23}, s_{23}} \sum_{L\rho, X} |\mathcal{G}_{L\rho X}^{j_{23}l_{23}s_{23}}(k_{23}, k)|^2, \quad (5)$$

where  $\mathbf{k}_{23}$  is the Cartesian momentum for the internal motion of the [23]-pair and  $\mathbf{k}$  the one of the probed nucleon in the intrinsic frame of the  $A = 3$  system,  $E_{23} = \sqrt{M_{23}^2 + \mathbf{k}^2}$ , with  $M_{23} = 2 \sqrt{m^2 + |\mathbf{k}_{23}|^2}$ ,  $k^+ = \xi M_0(1, 2, 3) \neq \kappa^+$ , with  $M_0(1, 2, 3)$  the free mass of the  $A = 3$  system, and  $E(\mathbf{k}) = \sqrt{m^2 + |\mathbf{k}|^2}$ . The nonsymmetric intrinsic variables  $\mathbf{k}$  and  $\mathbf{k}_{23}$  (see [14] for their definition) generate the relevant coefficients appearing in the integrand.

For  $A = 3$  one can immediately calculate the spin-independent LF-momentum distribution in Eq. (5), and then the light-cone momentum distributions,  $f_1^N(\xi)$ , Eq. (3). Analogously, one can evaluate the longitudinally and transversely polarized nucleon distributions,  $g_1^N$  and  $h_1^N$ , by using the spin-dependent nucleon momentum distribution,  $n_{\sigma, \sigma'}^N(\xi, \mathbf{k}_\perp, \mathbf{S})$ , i.e. the elements of  $\mathcal{N}_{\mathcal{M}}^N(\xi, \mathbf{k}_\perp, \mathbf{S})$  [15]. These distributions are given by

$$g_1^N(\xi) = \int d\mathbf{k}_\perp \Delta f^N(\xi, \mathbf{k}_\perp), \quad (6)$$

$$h_1^N(\xi) = \int d\mathbf{k}_\perp \Delta'_T f^N(\xi, \mathbf{k}_\perp), \quad (7)$$

where  $\Delta f^N(\xi, \mathbf{k}_\perp)$  and  $\Delta'_T f^N(\xi, \mathbf{k}_\perp)$  are two out of the six leading-twist transverse-momentum distributions [15]. In terms of  $\mathcal{N}_{\mathcal{M}}^N(\xi, \mathbf{k}_\perp, \mathbf{S})$  elements (for  $\mathcal{J} = 1/2$  the dependence upon  $\mathcal{M}$  amounts to a trivial phase [15]), one gets

$$g_1^N(\xi) = \int d\mathbf{k}_\perp \left[ n_{++}^N(\xi, \mathbf{k}_\perp, \hat{z}) - n_{--}^N(\xi, \mathbf{k}_\perp, \hat{z}) \right], \quad (8)$$

and

$$h_1^N(\xi) = \int d\mathbf{k}_\perp \left[ n_{+-}^N(\xi, \mathbf{k}_\perp, \hat{x}) + n_{-+}^N(\xi, \mathbf{k}_\perp, \hat{x}) \right], \quad (9)$$

where longitudinal and transverse-spin states are used, and one should recall that  $\mathbf{S} \parallel \hat{z}$  for  $g_1^N$  and  $\mathbf{S} \perp \hat{z}$  for  $h_1^N$ .

The distributions  $g_1^N(\xi)$  and  $h_1^N(\xi)$  are crucial for: i) evaluating inclusive spin-dependent SFs needed in the IA treatment of polarized DIS and devising a proper extraction method for collecting the neutron information from the  ${}^3\text{He}$  nucleus (see, e.g., Ref. [28] for the nonrelativistic (NR) case), and ii) analysing semi-inclusive DIS off transversely polarized  ${}^3\text{He}$  (see Refs. [29, 30] for the NR case), so that the neutron single-spin asymmetries can be obtained. Notice that the relativistic evaluation of these distributions is particularly relevant in view of the future measurements at high energy facilities, such as the EIC [8].

*Results.* For the first time, the nucleon momentum distributions given in Eqs. (3), (8) and (9) are evaluated for  ${}^3\text{He}$  within a fully Poincaré-covariant approach, by using wfs obtained along the line of Refs. [23, 24], and are shown in Figs. 1, 2 and 3, respectively. The difference between the longitudinally and transversely polarized distributions is a measure of the relevance of the relativistic effects, which appear to be more sizable for the proton than for the neutron, given that only small partial waves with high orbital angular momentum contribute to the tiny proton polarization in  ${}^3\text{He}$ . As expected,  $g_1^n$  and  $h_1^n$  are remarkably larger than the corresponding proton distributions.

To evaluate the nuclear SF from Eq. (2) both  $F_2^P$  and  $F_2^n$  are needed. Many parametrizations exist for  $F_2^P$  (see, e.g., Refs. [18, 31–33]) from proton experimental data, while  $F_2^n$  is elusive, due to the lack of free neutron targets. Thus, for  $F_2^n(x)$  we largely rely on experimental information provided by the new accurate data,  $E^{ht}(x) = \sigma^h/\sigma^t$ , from Ref. [9]. We also take into account the two results at  $x = 0$  and  $x = 1$  (with large uncertainties) obtained in Ref. [34] applying a careful extrapolation method to  $E^{ht}(x)$  [9]. Then we perform a quadratic least-squares interpolation of the experimental quantity  $E^{ht}(x)$  [9] plus the two extrapolated values [34], obtaining the function  $\mathcal{E}^{ht}(x)$  (cf. Fig. 1 in the Supplemental Material), which is necessary for adopting

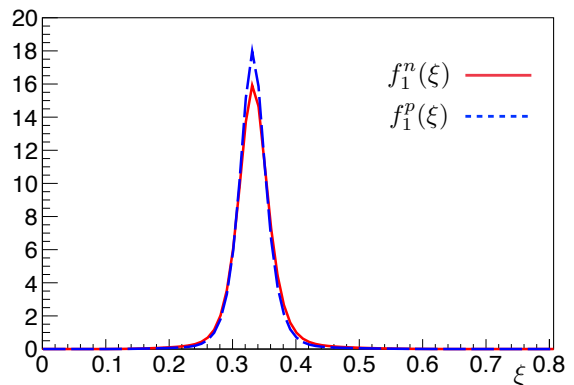


FIG. 1. (Color online). Light-cone momentum distributions, Eq. (3) for proton and neutron in  ${}^3\text{He}$ .

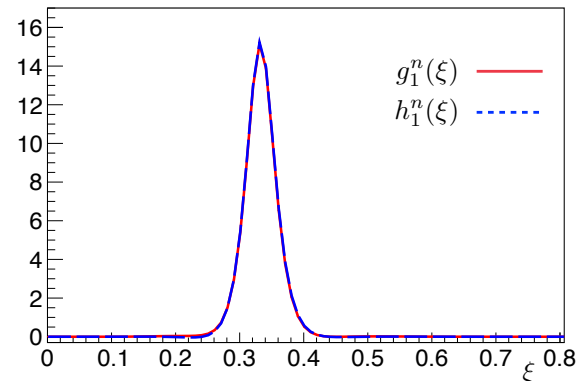


FIG. 2. (Color online). Light-cone helicity and transversity momentum distributions, Eqs. (8) and (9), for a neutron in  ${}^3\text{He}$ .

the iterative method presented in Refs. [16, 17] and eventually extracting  $r(x) = F_2^n(x)/F_2^p(x)$ .

Let us define the ratio

$$R_2^A(x) = \frac{F_2^A(x)}{Z F_2^p(x) + (A - Z) F_2^n(x)}, \quad (10)$$

and the super-ratio

$$R^{ht}(x) = \frac{R_2^{3He}(x)}{R_2^{3H}(x)} = E^{ht}(x) \frac{2r(x) + 1}{r(x) + 2}. \quad (11)$$

Noteworthy, in IA the super-ratio is a functional of  $r(x)$  ( $R^{ht}(x) = R^{ht}[x, r(x)]$ ), once a fixed parametrization for  $F_2^p(x)$  is used. Hence, the iterative method [16, 17] can be applied for determining the ratio  $r(x)$ , i.e.

$$r^{(n+1)}(x) = - \frac{\mathcal{E}^{ht}(x) - 2R^{ht}[x, r^{(n)}(x)]}{2\mathcal{E}^{ht}(x) - R^{ht}[x, r^{(n)}(x)]}, \quad (12)$$

where  $R^{ht}[x, r^{(n)}(x)] = R_2^{3He}[x, r^{(n)}(x)]/R_2^{3H}[x, r^{(n)}(x)]$  is obtained from our Poincaré-covariant calculations of Eq. (2) for the  $A = 3$  nuclei.

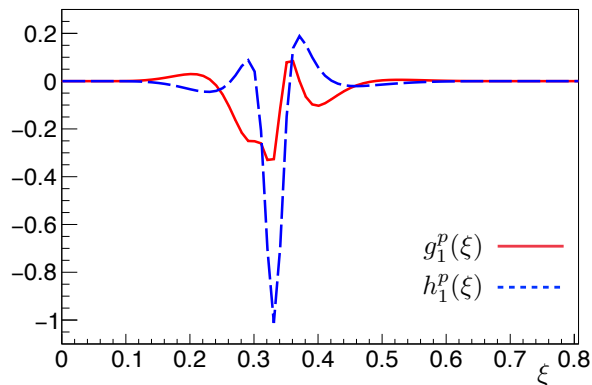


FIG. 3. (Color online). As in Fig. 2, but for a proton in  ${}^3\text{He}$ .

After assigning the initial  $r^{(0)}(x)$ , in the present calculation this quantity is built from  $F_2^{n(p)}$  of Ref. [18], one gets the results shown in Fig. 4 (notice that by using  $F_2^p(x)$  of Refs. [31–33] a similar final  $r(x)$  is achieved). There, the full dots represent stable outcomes, i.e. with a relative difference between the calculated ratios after 100 and 200 iterations less than 4‰. The uncertainties associated to our result (the shaded area) are attained by applying to the full dots both a quadratic least-squares interpolation and a cubic one, that corresponds to a better fit (see in the Supplemental Material the actual expressions). Moreover, in Fig. 4, our  $r(x)$  is compared with i) the data extracted by MARATHON [9] through Eq. (11) with the theoretical quantity  $R^{ht}(x)$  evaluated following Refs. [35, 36], and ii) the SMC  $r(x)$  ratio [18].

Once  $r(x)$  is determined, the nuclear structure functions of the iso-doublet, Eq. (2), are evaluated by using i) the parametrization for  $F_2^p(x)$  of Ref. [18], ii)  $F_2^n(x) = r(x)F_2^p(x)$ , and iii) the light-cone distributions from Eq. (3). In particular, after specializing to  $A = 3$  and  $A = 2$  the ratio in Eq. (10), one builds the EMC ratio for the three-body system, viz.

$$R_{EMC}^{3\text{He}(^3\text{H})}(x) = \frac{R_2^{3\text{He}(^3\text{H})}(x)}{R_2^{\text{D}}(x)}. \quad (13)$$

In Fig. 5 the comparison between the EMC experimental data for  ${}^3\text{He}$  [37], rescaled according to Ref. [36] (see also Ref. [9]) and the outcomes of our Poincaré-covariant approach (cf. Eq. (2)) is presented. The deuteron ratio  $R_2^{\text{D}}(x)$  has been evaluated by using the wf corresponding to the NN AV18 interaction and the expression of the LF deuteron SF consistent with Eq. (2) for  $A = 2$  (see Ref. [38]). For the  ${}^3\text{He}$  ratio, in order to study the dependence upon the nuclear interaction, we have adopted i) the  ${}^3\text{He}$  wf of Refs. [23, 24], corresponding to the charge dependent NN AV18 [25] interaction plus the NNN Urbana IX force [26], and ii) the one calculated without the NNN potential.

Let us emphasize that the calculations performed by

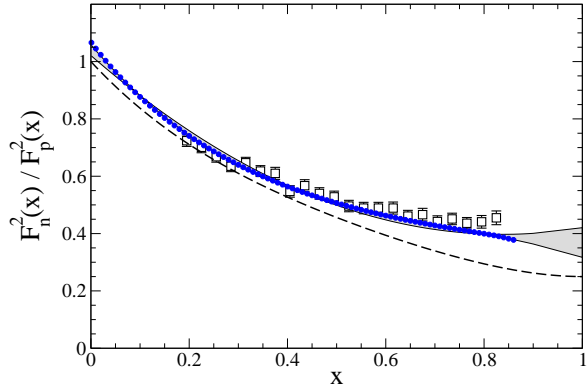


FIG. 4. The ratio  $r(x) = F_2^n(x)/F_2^p(x)$  obtained through the recurrence relation of Eq. (12), full dots (see text for the  $x$ -range), compared with i) the results extracted in Ref. [9], empty squares, and ii) the the ratio from the SMC  $F_2^{p(n)}(x)$  [18], dashed line. The shaded area is the uncertainty obtained by using i) a quadratic least-squares interpolation of the full-dot set and ii) a cubic one (see text).

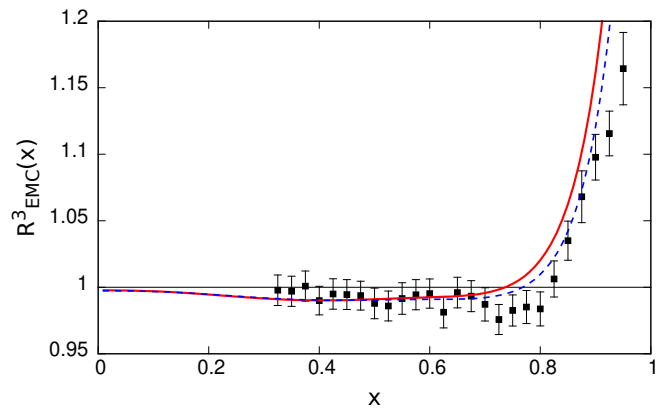


FIG. 5. The EMC ratio in  ${}^3\text{He}$ . Solid line: our calculation with i)  $F_2^p(x)$  of Ref. [18], ii)  $F_2^n(x) = r(x)F_2^p(x)$ , where  $r(x)$  has been determined through Eq. (12) and iii) the light-cone distributions corresponding to the NN AV18 [25] interaction plus the NNN Urbana IX force [26]. Dashed line: the same as the solid line, but excluding the NNN potential. Black squares: Jlab data of Ref. [37], as reanalysed in Ref. [36]. The uncertainties on  $r(x)$ , shown in Fig. 4, are fully absorbed by the width of the lines.

using the SMC  $F_2^{p(n)}(x)$  [18] cannot be distinguished by the calculations with our results for  $r(x)$  and that also the uncertainties affecting our  $r(x)$  for  $x > 0.85$  (see Fig. 4) have no visible effect in Fig. 5.

It is rewarding to notice that, for  $0.2 \leq x \leq 0.75$ , the calculated  ${}^3\text{He}$  EMC ratio becomes less than 1, without

any dynamical off-shell correction. This interesting result is generated by a clear, although small, combined effect of the careful treatment of the Poincaré covariance, the use of nonsymmetric variables to comply with macroscopic locality (cfr. Eq. (5)) and, last but not least, a realistic description of  ${}^3\text{He}$ . Moreover, Fig. 5 shows that the effect of the NNN interaction can be safely disregarded for  $x \leq 0.7$ . We also checked that the effects of Coulomb interaction and charge-dependence of the NN Av18 potential are tiny and can be disregarded.

Finally, Fig. 6 shows the comparison between the super-ratio  $R^{ht}(x)$ , Eq. (11), calculated in our approach and the same quantity extracted by MARATHON [9] by using the theoretical inputs of Refs. [35, 36]. The black area is generated by our calculations, corresponding to the quadratic least-squares interpolation of the full dots in Fig. 4 and the cubic one, respectively. It provides a clear insight into the expected impact of  $F_2^n(x) = r(x) F_2^p(x)$  on the  ${}^3\text{H}$  SF. It is worth noticing that a super-ratio with a similar pattern, i.e. definitely bending for  $x > 0.7$ , have been extracted i) through a global analysis by JAM Collaboration [10], ii) by using off-shell corrections obtained from Monte-Carlo fits in Ref. [39] (in the same work the super-ratio changes derivative once the off-shell corrections from Ref. [35] are adopted) and iii) in Ref. [40] where a universal modification of nucleons in short-range correlated pairs is considered.

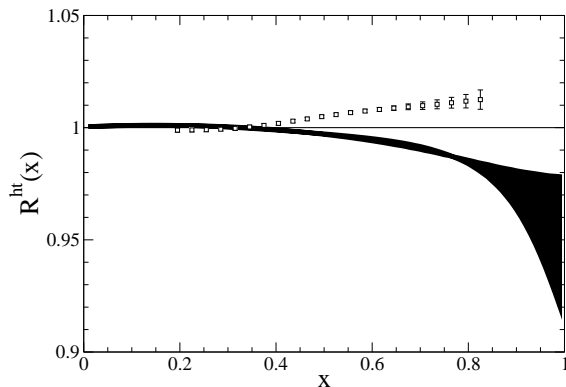


FIG. 6. The super-ratio  $R^{ht}(x)$ , Eq. (11). The black area represents our results obtained by using both a quadratic interpolation of the full dots in Fig. 4 and a cubic one. Empty squares: super-ratio obtained in Ref. [9] by using the approach of Refs. [35, 36] for the theoretical inputs.

*Conclusions.* A rigorous approach, elaborated within the light-front Hamiltonian dynamics, satisfying i) Poincaré covariance, ii) the baryon number sum rule, iii) the momentum sum rule and iv) the macroscopic locality,

is applied for the first time to the description of electron inclusive DIS off  $A = 3$  nuclei, obtaining the expected signature of the EMC effect, without medium deformations of the bound nucleons. We have adopted the Bjorken limit, and used very accurate nuclear wfs [23, 24], with a rich content of NN and NNN correlations, also checking the stability of the result against the use of different nuclear interactions (NN+NNN or NN only). In this way, within a Poincaré-covariant approach, we are able to set a baseline for starting a consistent separation of the genuinely nuclear effects (where the nucleon dof are acting) from the ones basically pertaining to QCD. with a direct impact on analysis and interpretation of future experimental results at the EIC.

The generalisation to  $A > 3$  nuclei, where the EMC effect is more pronounced, e.g. the  ${}^4\text{He}$  nucleus [37], is straightforward (although numerically challenging), since, in the Bjorken limit, only the momentum space wf is needed, as shown in Eqs. (2) and (3), valid for any nucleus.

*Acknowledgment.* M.R. and S.S. thank for the financial support received under the STRONG-2020 project of the European Union's Horizon 2020 research and innovation programme: Fund no 824093.

### Supplemental Material

In Fig. 7, the experimental ratio measured by the MARATHON Collaboration [9], with very small error bars, and the two values extrapolated at  $x = 0$  and  $x = 1$  of Ref. [34], with large uncertainties, are shown. The solid line is a quadratic interpolation obtained by using a least-squares method. The quadratic parametrization, indicated as  $\mathcal{E}^{ht}(x)$ , is adopted in the recurrence expression of Eq. (12) of the main text, because of the necessity to cover the full range of  $x$  for evaluating the theoretical super-ratio  $R^{ht}[x, r^{(n)}(x)]$  (cf. Eqs. (11), (10) and (2) in the main text).

In Fig. 4 of the main text the uncertainties depicted by the shaded area are obtained by using both a quadratic least-squares interpolation of the full dots, given by

$$r^q(x) = 1.02107 - 1.48834 x + 0.887864 x^2 ,$$

and a cubic one, given by

$$r^c(x) = 1.05835 - 1.99892 x + 2.31339 x^2 - 1.0557 x^3 .$$

Of course the best interpolation is obtained by using the cubic polynomial.

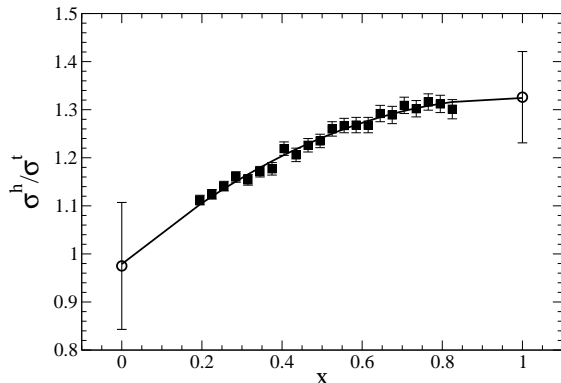


FIG. 7. The ratio  $\sigma^h/\sigma^t$  of inclusive DIS cross sections off  ${}^3\text{He}$  and  ${}^3\text{H}$ . Black squares: experimental data from Ref. [9]. Empty circles: extrapolated values as given in Ref. [34]. Solid line: quadratic least-squares interpolation.

- 
- [1] J. J. Aubert *et al.* (European Muon), “The ratio of the nucleon structure functions  $F_2^n$  for iron and deuterium,” *Phys. Lett. B* **123**, 275–278 (1983).  
 [2] O. Hen, G. A. Miller, E. Piassetzky, and L. B. Weinstein, “Nucleon-Nucleon Correlations, Short-lived Excitations, and the Quarks Within,” *Rev. Mod. Phys.* **89**, 045002 (2017), arXiv:1611.09748 [nucl-ex].

- [3] B. Schmookler *et al.* (CLAS), “Modified structure of protons and neutrons in correlated pairs,” *Nature* **566**, 354–358 (2019), arXiv:2004.12065 [nucl-ex].  
 [4] X. G. Wang, A. W. Thomas, and W. Melnitchouk, “Do short-range correlations cause the nuclear EMC effect in the deuteron?” *Phys. Rev. Lett.* **125**, 262002 (2020), arXiv:2004.03789 [hep-ph].  
 [5] I. C. Cloët *et al.*, “Exposing Novel Quark and Gluon Effects in Nuclei,” *J. Phys. G* **46**, 093001 (2019), arXiv:1902.10572 [nucl-ex].  
 [6] R. Dupré and S. Scopetta, “3D Structure and Nuclear Targets,” *Eur. Phys. J. A* **52**, 159 (2016), arXiv:1510.00794 [nucl-ex].  
 [7] W. Armstrong *et al.*, “Tagged EMC Measurements on Light Nuclei,” (2017), arXiv:1708.00891 [nucl-ex].  
 [8] R. Abdul Khalek *et al.*, “Science Requirements and Detector Concepts for the Electron-Ion Collider: EIC Yellow Report,” (2021), arXiv:2103.05419 [physics.ins-det].  
 [9] D. Abrams *et al.* (MARATHON), “Measurement of the Nucleon  $F_2^n/F_2^p$  Structure Function Ratio by the Jefferson Lab MARATHON Tritium/Helium-3 Deep Inelastic Scattering Experiment,” *Phys. Rev. Lett.* **128**, 132003 (2022), arXiv:2104.05850 [hep-ex].  
 [10] C. Cocuzza, C. E. Keppel, H. Liu, W. Melnitchouk, A. Metz, N. Sato, and A. W. Thomas (Jefferson Lab Angular Momentum (JAM)), “Isovector EMC Effect from Global QCD Analysis with MARATHON Data,” *Phys. Rev. Lett.* **127**, 242001 (2021), arXiv:2104.06946 [hep-ph].  
 [11] Emanuele Pace, Matteo Rinaldi, Giovanni Salmè, and Sergio Scopetta, “EMC effect, few-nucleon systems and Poincaré covariance,” *Phys. Scripta* **95**, 064008 (2020), arXiv:2004.05877 [nucl-th].  
 [12] Paul A. M. Dirac, “Forms of Relativistic Dynamics,” *Rev. Mod. Phys.* **21**, 392–399 (1949).  
 [13] B. D. Keister and W. N. Polyzou, “Relativistic Hamiltonian dynamics in nuclear and particle physics,” *Adv. Nucl. Phys.* **20**, 225–479 (1991).  
 [14] Alessio Del Dotto, Emanuele Pace, Giovanni Salmè, and Sergio Scopetta, “Light-Front spin-dependent Spectral Function and Nucleon Momentum Distributions for a Three-Body System,” *Phys. Rev. C* **95**, 014001 (2017), arXiv:1609.03804 [nucl-th].  
 [15] Rocco Alessandro, Alessio Del Dotto, Emanuele Pace, Gabriele Perna, Giovanni Salmè, and Sergio Scopetta, “Light-front transverse momentum distributions for  $J=1/2$  hadronic systems in valence approximation,” *Phys. Rev. C* **104**, 065204 (2021), arXiv:2107.10187 [nucl-th].  
 [16] E. Pace, G. Salmè, and S. Scopetta, “Neutron unpolarized structure function  $F_2^N(x)$  from deep inelastic scattering off  ${}^3\text{He}$  and  ${}^3\text{H}$ ,” *Nucl. Phys. A* **689**, 453–456 (2001), arXiv:nucl-th/0009028.  
 [17] E. Pace, G. Salmè, S. Scopetta, and A. Kievsky, “Neutron structure function  $F(2)^{*n}(x)$  from deep inelastic electron scattering off few nucleon systems,” *Phys. Rev. C* **64**, 055203 (2001), arXiv:nucl-th/0109005.  
 [18] B. Adeva *et al.* (Spin Muon Collab. (SMC)), “The Spin dependent structure function  $g_1(x)$  of the proton from polarized deep inelastic muon scattering,” *Phys. Lett. B* **412**, 414–424 (1997).  
 [19] Jason Robert Smith and Gerald A. Miller, “Return of the EMC effect: Finite nuclei,” *Phys. Rev. C* **65**, 055206 (2002), arXiv:nucl-th/0202016.

- [20] Gerald A. Miller and Jason Robert Smith, “Return of the EMC effect,” *Phys. Rev. C* **65**, 015211 (2002), [Erratum: *Phys.Rev.C* 66, 049903 (2002)], arXiv:nucl-th/0107026.
- [21] U. Oelfke, P. U. Sauer, and F. Coester, “Convolution models of deep inelastic scattering: The Three nucleon bound states as a test case,” *Nucl. Phys. A* **518**, 593–616 (1990).
- [22] F. Coester, “Null plane dynamics of particles and fields,” *Prog. Part. Nucl. Phys.* **29**, 1–32 (1992).
- [23] A. Kievsky, M. Viviani, and S. Rosati, “Study of bound and scattering states of three nucleon systems,” *Nucl. Phys. A* **577**, 511–527 (1994), arXiv:nucl-th/9706067.
- [24] A. Kievsky, M. Viviani, and S. Rosati, “Cross-section, polarization observables, and phase shift parameters in proton deuteron and neutron deuteron elastic scattering,” *Phys. Rev. C* **52**, R15–R19 (1995).
- [25] Robert B. Wiringa, V. G. J. Stoks, and R. Schiavilla, “An Accurate nucleon-nucleon potential with charge independence breaking,” *Phys. Rev. C* **51**, 38–51 (1995), arXiv:nucl-th/9408016.
- [26] B. S. Pudliner, V. R. Pandharipande, J. Carlson, and Robert B. Wiringa, “Quantum Monte Carlo calculations of  $A \leq 6$  nuclei,” *Phys. Rev. Lett.* **74**, 4396–4399 (1995), arXiv:nucl-th/9502031.
- [27] F. M. Lev, E. Pace, and G. Salmè, “Electromagnetic and weak current operators for interacting systems within the front form dynamics,” *Nucl. Phys. A* **641**, 229–259 (1998), arXiv:hep-ph/9807255.
- [28] Claudio Ciofi degli Atti, S. Scopetta, E. Pace, and G. Salmè, “Nuclear effects in deep inelastic scattering of polarized electrons off polarized He-3 and the neutron spin structure functions,” *Phys. Rev. C* **48**, R968–R972 (1993), arXiv:nucl-th/9303016.
- [29] Sergio Scopetta, “Neutron single spin asymmetries from semi-inclusive deep inelastic scattering off transversely polarized He-3,” *Phys. Rev. D* **75**, 054005 (2007), arXiv:hep-ph/0612354.
- [30] L. P. Kaptari, A. Del Dotto, E. Pace, G. Salmè, and S. Scopetta, “Distorted spin-dependent spectral function of an  $A=3$  nucleus and semi-inclusive deep inelastic scattering processes,” *Phys. Rev. C* **89**, 035206 (2014), arXiv:1307.2848 [nucl-th].
- [31] J. J. Aubert *et al.* (European Muon), “Measurements of the nucleon structure functions  $F_2^n$  in deep inelastic muon scattering from deuterium and comparison with those from hydrogen and iron,” *Nucl. Phys. B* **293**, 740–786 (1987).
- [32] M. Gluck, E. Reya, and A. Vogt, “Parton distributions for high-energy collisions,” *Z. Phys. C* **53**, 127–134 (1992).
- [33] Alan D. Martin, R. G. Roberts, W. J. Stirling, and R. S. Thorne, “MRST2001: Partons and  $\alpha_s$  from precise deep inelastic scattering and Tevatron jet data,” *Eur. Phys. J. C* **23**, 73–87 (2002), arXiv:hep-ph/0110215.
- [34] Zhu-Fang Cui, Fei Gao, Daniele Binosi, Lei Chang, Craig D. Roberts, and Sebastian M. Schmidt, “Valence Quark Ratio in the Proton,” *Chin. Phys. Lett.* **39**, 041401 (2022), arXiv:2108.11493 [hep-ph].
- [35] Sergey A. Kulagin and R. Petti, “Global study of nuclear structure functions,” *Nucl. Phys. A* **765**, 126–187 (2006), arXiv:hep-ph/0412425.
- [36] S. A. Kulagin and R. Petti, “Structure functions for light nuclei,” *Phys. Rev. C* **82**, 054614 (2010), arXiv:1004.3062 [hep-ph].
- [37] J. Seely *et al.*, “New measurements of the EMC effect in very light nuclei,” *Phys. Rev. Lett.* **103**, 202301 (2009), arXiv:0904.4448 [nucl-ex].
- [38] E. Pace and G. Salmè, “Deuteron electromagnetic properties with a Poincare covariant current operator within front form Hamiltonian dynamics,” in *8th Conference on Problems in Theoretical Nuclear Physics* (2001) arXiv:nucl-th/0106004.
- [39] A. J. Tropiano, J. J. Ethier, W. Melnitchouk, and N. Sato, “Deep-inelastic and quasielastic electron scattering from  $A = 3$  nuclei,” *Phys. Rev. C* **99**, 035201 (2019), arXiv:1811.07668 [nucl-th].
- [40] E. P. Segarra, A. Schmidt, T. Kutz, D. W. Higinbotham, E. Piassetzky, M. Strikman, L. B. Weinstein, and O. Hen, “Neutron Valence Structure from Nuclear Deep Inelastic Scattering,” *Phys. Rev. Lett.* **124**, 092002 (2020), arXiv:1908.02223 [nucl-th].